

# Synthesis under $\text{NH}_3$ and thermal behaviour of $\text{SiCNAIO}$ 2 polymer-derived nanopowders

Vincent Salles\*, Sylvie Foucaud, Paul Goursat, Eric Champion

SPCTS, UMR CNRS 6638, Faculté des Sciences, 123 Avenue Albert Thomas, 87060 Limoges, France

Received 24 May 2007; received in revised form 19 September 2007; accepted 30 September 2007

Available online 3 December 2007

## Abstract

The influence of a reactive atmosphere ( $\text{Ar}/\text{NH}_3$ ) on the composition of  $\text{SiCNAIO}$  powders was studied at  $1400^\circ\text{C}$ , with a total gas flow rate of  $3\text{ L min}^{-1}$  and an ammonia content of 0–25 vol.%. Powders with a large range of carbon amount (3–23 wt.%) were synthesized at  $1400^\circ\text{C}$  in a  $\text{Ar}/\text{NH}_3$  atmosphere. Elemental analyses showed that in reducing conditions, the presence of reacting species in the heating zone implied the nitridation of the system, with amounts of nitrogen included in the range 35–47 wt.%. The thermal stability of the different batches was then tested by TGA experiments, up to  $1550^\circ\text{C}$  in a  $\text{N}_2/\text{He}$  mixture. For  $\text{C}/\text{N} \geq 0.8$ , the powder thermal stability is limited and the main crystalline phase is  $\beta\text{-SiC}$ . On the contrary, for  $\text{C}/\text{N} < 0.8$ , the powder mass loss is negligible and both  $\alpha$ - and  $\beta\text{-Si}_3\text{N}_4$  are detected after the heat-treatment. The sinterability of such powders was evaluated by preliminary tests, a higher shrinkage of the pellets, containing aluminum and oxygen elements, was evidenced.

© 2007 Elsevier Ltd. All rights reserved.

**Keywords:** Powders-chemical preparation; Nanocomposites;  $\text{Si}_3\text{N}_4/\text{SiC}$ ; Thermal properties

## 1. Introduction

The pyrolysis of molecular precursors is a promising route for the elaboration of technical ceramics, and a lot of recent papers deal with this synthesis method.<sup>1–5</sup> The interest of this approach is the fabrication of near net-shape products, with a high purity, or the fabrication of homogeneous multielement materials. In the case of the silicon carbonitride system, many studies were carried out on the synthesis of preceramic polymers containing heteroelements such as Ti,<sup>6</sup> Fe,<sup>7</sup> Y,<sup>8</sup> Al<sup>9–14</sup> and B.<sup>5,15–22</sup> Up to now, fully dense materials have been very difficult to obtain by a direct pyrolysis of the polymer due to the important gaseous release occurring during the thermal treatment.<sup>8,10,13,16,17</sup> To avoid this phenomenon, we have first intended to produce ultrafine powders by pyrolysis of a molecular precursor and then to densify the as-prepared powders using a suitable heat-treatment. The synthesis of prealloyed powders containing Si/C/N/Al/(O) elements, realized by the thermal spray-pyrolysis of an organometallic precursor called “alumi-

nosilazane”, is described in a previous paper.<sup>23</sup> The control of the pyrolysis parameters, like the furnace temperature and the gas flow rate, allowed to produce powders having a higher thermal stability than that synthesized by laser pyrolysis under similar conditions.<sup>24,25</sup> In our case, particles of 30–200 nm were obtained according to the total gas flow rate used ( $1\text{–}6\text{ L min}^{-1}$ ). They were amorphous and had a tunable composition. After pyrolysis under pure argon, it was evidenced that free carbon was present in all the batches. A test realized under a reactive atmosphere ( $\text{Ar}/\text{NH}_3$ ) showed a drop in carbon content whereas the amount of aluminum increased.

In the present work, we have synthesized several batches of powders using different  $\text{NH}_3$  rates in the pyrolysis atmosphere. Then, the thermal behaviour and the sinterability of the prealloyed powders were studied according to their composition.

## 2. Experimental details

### 2.1. Powders synthesis

The precursor and the powder synthesis were both detailed elsewhere.<sup>23</sup> The organometallic precursor (aluminosilazane) is formed after reaction between trimethylaluminum

\* Corresponding author. Tel.: +33 5 55 45 74 61; fax: +33 5 55 45 75 86.  
E-mail address: [vincent.salles@unilim.fr](mailto:vincent.salles@unilim.fr) (V. Salles).

(TMA =  $(\text{CH}_3)_3\text{Al}$ , Aldrich) and hexamethyldisilazane (HMDS =  $(\text{Si}(\text{CH}_3)_3)_2\text{NH}$ , Aldrich) at room temperature, in an inert atmosphere. In this paper, two contents of aluminum in the aluminosilazane, corresponding to Si/Al molar ratios of 30 and 15, are considered. In such conditions, the precursor remains liquid, which is necessary to form an aerosol into the spray-pyrolysis device. The droplets are carried to the furnace using argon gas. Then, the precursor decomposes in the reactional zone generating gaseous species, which recondense in ultrafine powders while cooling. The particles are finally trapped into two collectors placed before the vacuum pump. The influence of the reactive atmosphere was studied using different contents of ammonia in the range of 0–25 vol.%. The total gas flow rate was fixed at  $3 \text{ L min}^{-1}$ , except for one sample ( $6 \text{ L min}^{-1}$ ), and the main part of the experiments was carried out at  $1400^\circ\text{C}$ . After the synthesis, all the powders were stored into a glove box under argon.

Different analytical techniques were used for the characterization: SEM observations (Philips XL 30, powders were scattered in an ethanol solution, using a drop of the suspension for observation after solvent evaporation), specific surface area measurements (Micromeritics—ASAP 2010, BET 8 pts,  $\text{N}_2$ ), X-ray diffraction measurements (Siemens, D5000,  $2\theta$ ,  $\text{Cu K}\alpha_1$ ), FTIR spectroscopy (Spectrum One FTIR, Perkin-Elmer, using KBr pellets method),  $^{29}\text{Si}$ ,  $^{27}\text{Al}$  and  $^{13}\text{C}$  NMR spectroscopy (Brüker spectrometer, 400 MHz/89 mm, Service de RMN du solide, GDPC, Université de Montpellier II). For elemental analysis (Service Central d'Analyse du CNRS, Vernaison, France), Si and Al were analysed by ICP-AES technique after chemical dissolution, C by combustion to  $1800^\circ\text{C}$  under oxygen, and N by pyrolysis to  $3000^\circ\text{C}$  under He in a graphite crucible.

## 2.2. Thermal stability and sintering

The thermal stability of the as-synthesized powders was determined by thermogravimetric analysis (TGA) (Setaram, B60). The experiments were carried out on powders, to emphasize the phenomena occurring during the thermal treatment, under a dynamic gas mixture ( $\text{N}_2/\text{He}$ , 20/80 vol.%, 99.999% purity) at a flow rate of  $0.08 \text{ L min}^{-1}$ , to compare our results with previous works.<sup>24</sup> The samples (30–50 mg) were heated in  $\text{Al}_2\text{O}_3$  crucibles up to  $1550^\circ\text{C}$ , with a heating rate of  $10^\circ\text{C min}^{-1}$ , and a dwell time of 2 h. After the heat-treatment, the crystalline phases of the samples were identified by X-ray diffraction.

A preliminary study on the sintering behaviour was carried out in order to establish the relationship between the chemical composition and the densification rate, and finally to refine the

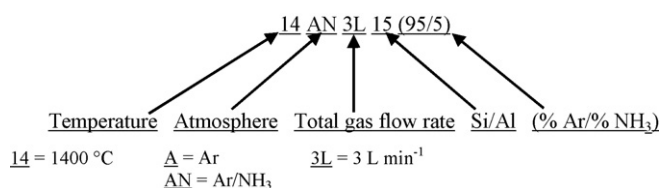


Fig. 1. Nomenclature established according the pyrolysis conditions.

pyrolysis parameters. The as-pyrolysed powders were put into a 12 mm diameter graphite die and hot-pressed at 35 MPa (200LC, LPA). The aim was to compare the behaviour of these powders to that of synthesized in preliminary studies. The thermal treatment was composed of a heating rate of  $15^\circ\text{C min}^{-1}$ , a dwell temperature at  $1650^\circ\text{C}$  during 2 h, a cooling rate of  $20^\circ\text{C min}^{-1}$ .

X-ray diffraction (XRD) was conducted on the cross-sections parallel to the direction of the applied pressure.

## 3. Results and discussion

### 3.1. Synthesis of powders under argon/ammonia

The presence of free carbon in the  $\text{Si}_3\text{N}_4/\text{SiC}$  powders has a deleterious effect on the sintering behaviour. Different previous studies, dealing with polysilazane and polycarbosilane pyrolysis, showed that the introduction of ammonia into the pyrolysis atmosphere leads to a decrease of the final carbon content.<sup>25–29</sup> In this work, pyrolysis experiments were carried out in a reactive atmosphere ( $\text{Ar}/\text{NH}_3$ ), with different amounts of ammonia: 5, 10, 15 and 25 vol.%. All the batches were fabricated with the same aluminum content, corresponding to a Si/Al molar ratio of 15 in the starting aluminosilazane (nomenclature in Fig. 1).

The presence of nitriding species and hydrogen into the pyrolysis atmosphere implies colour changes of the powders. They are lighter as the rate of  $\text{NH}_3$  increases. Moreover, the particles ( $\phi_{\text{part}}$ , calculated as in previous works<sup>23</sup>) are smaller when an argon/ammonia mixture is used, as indicated in Table 1. Therefore, the values of the specific surface area ( $S_{\text{BET}}$ ) increase from 29 to  $69 \text{ m}^2 \text{ g}^{-1}$ , respectively from 0 to 15 vol.% of ammonia in argon. They do not change for rates of  $\text{NH}_3$  higher than 15%, this could be due to the atmosphere saturation by nitriding species. The amorphous state of powders is confirmed in both cases by XRD, with or without ammonia.

The carbon content was measured by chemical analysis (Table 2). The introduction of ammonia into the pyrolysis atmosphere leads to a decrease of carbon content from 46 to 3 wt.% when the  $\text{NH}_3$  rate evolves from 0 to 25 vol.%. This carbon

Table 1  
Specific surface area and calculated particle size according to rates of ammonia in the pyrolysis atmosphere

	Powder batches				
	14A3L15	14AN3L15 (95/5)	14AN3L15 (90/10)	14AN3L15 (85/15)	14AN3L15 (75/25)
% $\text{NH}_3$	0	5	10	15	25
$S_{\text{BET}}$ ( $\text{m}^2 \text{ g}^{-1}$ )	29	34	41	69	70
$\phi_{\text{part}}$ <sup>a</sup>	86	73	61	36	36

<sup>a</sup>  $\phi_{\text{part}}$  (nm) =  $6000/(d_{\text{th}}S_{\text{BET}})$ ; with  $d_{\text{th}} = 2.4$  and  $S_{\text{BET}}$  expressed in  $\text{m}^2 \text{ g}^{-1}$ .

Table 2  
Chemical composition of the nanopowders according to the pyrolysis atmosphere

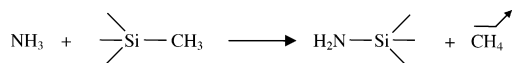
Batches	Composition (wt.%)					Molar ratio							
	Si	C	N	Al	O	C/N		C/Si		Si/N		Si/Al	
						th. <sup>a</sup>	final <sup>b</sup>	th.	final	th.	final	th.	final
14A3L15	36.6	45.8	11.9	0.5	0.6	6.4	4.5	3.2	2.9	2.0	1.5	15.0	70.3
14AN3L15 (95/5)	47.3	22.5	34.8	1.5	0.6	"	0.8	"	1.1	"	0.7	"	30.3
14AN3L15 (90/10)	49.2	12.5	35.0	1.4	3.3	"	0.4	"	0.6	"	0.7	"	33.8
14AN3L15 (85/15)	51.6	4.6	37.0	1.2	5.2	"	0.1	"	0.2	"	0.7	"	41.3
14AN3L15 (75/25)	44.6	3.4	46.6	0.9	5.1	"	0.1	"	0.2	"	0.5	"	47.6

<sup>a</sup> th. = theoretical ratio contained in the precursor.

<sup>b</sup> final = ratio calculated from elemental analyses of the powders.

release is responsible for the grey colour of the powders synthesized in Ar/NH<sub>3</sub> atmosphere. It was previously shown that the decomposition of silazane precursors occurs in the range 450–800 °C.<sup>28,30</sup> The Si–N bond being more stable than the Si–C one, regarding the bond energies, we can suggest that the cleavage of the Si–C bonds occurs at first, leading to the formation of silicon-based radicals and to the release of gaseous species such as CH<sub>4</sub> and C<sub>2</sub>H<sub>6</sub>. The presence of ammonia in such conditions would lead to the formation of Si–NH<sub>2</sub> groups as proposed in previous works (Scheme 1).<sup>31</sup> This mechanism corresponds to a nucleophilic attack of molecular ammonia on silicon-based radicals.<sup>27,31</sup> Other investigations evidenced a decreasing carbon content with an increasing amount of H<sub>2</sub> in the pyrolysis atmosphere.<sup>32</sup> The decomposition of ammonia, leading to the formation of N<sub>2</sub>, NH<sub>x</sub> species<sup>33</sup> and H<sub>2</sub>, could also participate to the cleavage of Si–C bonds. Taking into account previous works, it seems difficult to exactly know the decomposition rate of NH<sub>3</sub>, since the thermodynamic and the kinetic aspects, must be considered.<sup>33,34</sup> In the pyrolysis device, the ammonia is introduced into the furnace at 1000 °C, and finally a carbon loss accompanied by a nitrogen gain are observed. Thermodynamically, molecular NH<sub>3</sub> does not exist anymore above 700 °C,<sup>33</sup> and a reaction with molecular nitrogen is impossible up to 1300–1400 °C. We observed a nitridation of the powders so the decomposition of ammonia is not complete when NH<sub>3</sub> is introduced. Moreover, Rice et al. showed that a lot of gaseous species are produced when hexamethyldisilazane decomposes.<sup>35</sup> Therefore, complex reactions must occur in the reactional zone, so it is difficult to propose a precise pyrolysis mechanism.

The nitrogen content is stabilized around 35 wt.% for 5–15 vol.% of NH<sub>3</sub>. This corresponds to a molar ratio Si/N = 0.7 which is close to the value (Si/N = 0.75) in the Si<sub>3</sub>N<sub>4</sub> material. For an atmosphere containing 25 vol.% of ammonia, the molar ratio Si/N = 0.5 would mean that the powders contain a nitrogen excess. Fig. 2 presents FT-IR spectra of as-pyrolysed powders in different rates of ammonia (0, 5 and 25%). For powders pyrolysed in a reactive atmosphere, spectra show new bands: C–N (1300 cm<sup>-1</sup>), C=N (1600 cm<sup>-1</sup>) and C≡N (2200 cm<sup>-1</sup>).



Scheme 1.

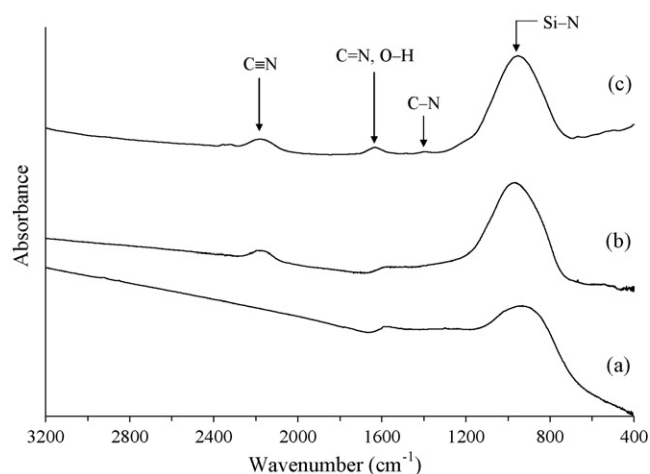


Fig. 2. FT-IR spectra of powders synthesized under different rates of ammonia in the pyrolysis atmosphere: (a) 0%, (b) 5% and (c) 25% of NH<sub>3</sub> in Ar (vol.%).

The high nitrogen content could be explained by the presence of such bonds between C and N which have been already evidenced in previous works.<sup>36–38</sup> Therefore, we can suggest that the most part of the carbon contained in the powders is free carbon, but there is a non-negligible amount of carbon linked to nitrogen. The band at 1600 cm<sup>-1</sup> could also correspond to O–H bonds, due to the presence of water adsorbed on the particles surface during their handling. Very small content of hydrogen, detected by chemical analysis of the powders, could be attributed to the hydrolysis of the particle surface. Groups like Si–NH<sub>2</sub> are excluded above 300 °C in the pyrolysis atmosphere.<sup>39</sup>

Table 2 also shows aluminum content changes with the ammonia rate. The reactive atmosphere allows to stabilize the Al–N bond into the reactional zone but an ammonia amount superior to 5% leads to an increasing loss of aluminum.<sup>40</sup> Experiments are in progress to explain this phenomenon. Nevertheless, an Ar/NH<sub>3</sub> mixture allows minimizing the loss of aluminum.

<sup>29</sup>Si NMR spectroscopy (Fig. 3) clearly evidences a nitridation process of the powders. Ammonia introduction leads to an elemental environment modification. An argon pyrolysis atmosphere favours carbon-rich environments, such as SiC<sub>4</sub>/SiC<sub>2</sub>N<sub>2</sub> (–20 ppm), whereas an Ar/NH<sub>3</sub> mixture leads to nitrogen-rich environments, such as SiCN<sub>3</sub> and SiN<sub>4</sub> (around –35 and –50 ppm).<sup>41</sup> Peaks are progressively centred around –50 ppm as the ammonia rate increases.

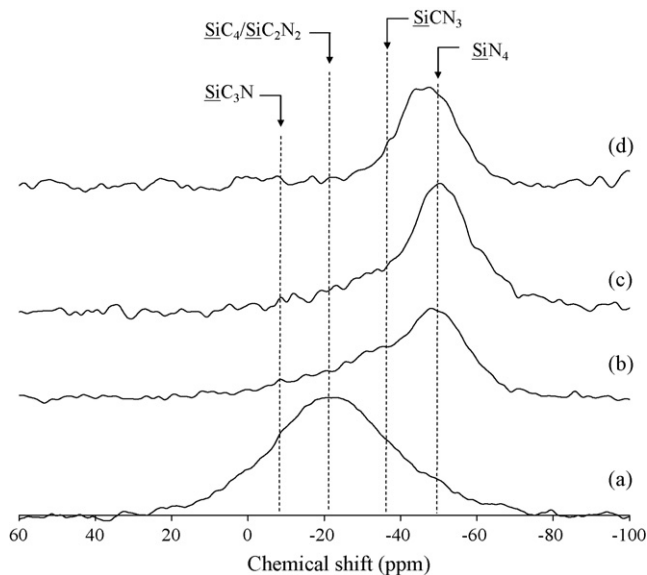


Fig. 3.  $^{29}\text{Si}$  NMR spectra of powders synthesized under different rates of ammonia in the pyrolysis atmosphere: (a) 0%, (b) 5%, (c) 10% and (d) 15% of  $\text{NH}_3$  in Ar (vol.%).

The aluminum and oxygen contents being low, compositional changes of powders can be summarized in the Si/C/N ternary diagram presented in Fig. 4. The influence of the total flow rate and the decrease of carbon content in the powders were previously studied, using two values: 1 or  $3 \text{ L min}^{-1}$ .<sup>23</sup> So all the results show that, under the pyrolysis conditions used, it seems difficult to reach the  $\text{Si}_3\text{N}_4/\text{SiC}$  binary system. For all the rates of ammonia, the powder composition only evolves along the  $\text{Si}_3\text{N}_4/\text{C}$  binary system. Whatever the ammonia rate, the N/H ratio introduced in the reactional zone remains constant. In these

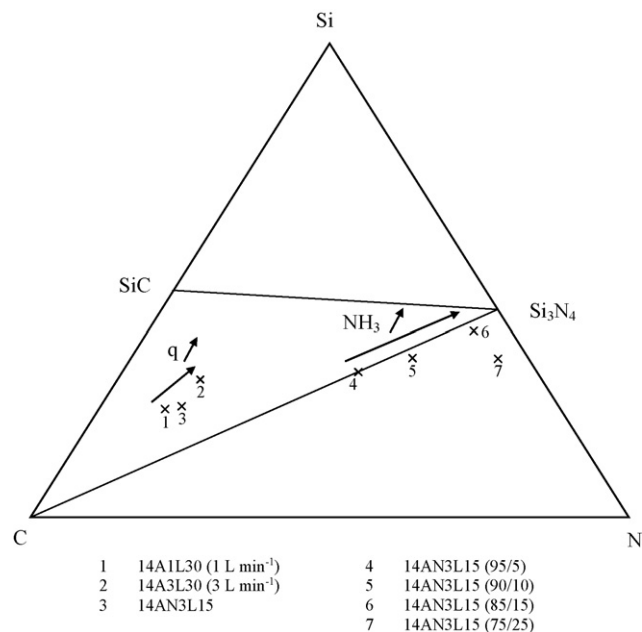


Fig. 4. Si–C–N ternary diagram involving the powder composition changes according to the total gas flow rate ( $q$ ) and the rate of ammonia ( $\text{NH}_3$ ) in the pyrolysis atmosphere.

conditions, the proportion of the nitrogen fixed into the powders and the proportion of the carbon loss are linked. In so far as the polyaluminosilazane contains a lot of carbon ( $\text{C/N} \geq 6$ ) before the pyrolysis step, the cleavage of  $\text{Si-CH}_x$  bonds without nitrification is limited in these conditions. Experiments are in progress under a more reducing pyrolysis atmosphere for a better control of the carbon and nitrogen contents.

### 3.2. Thermal behaviour

The behaviour at high temperature of the as-pyrolysed powders was studied by TGA. Only powder beds were used to emphasize the phenomena due to the thermal treatments. The aim was to determine the more suitable composition for the material densification.

#### 3.2.1. Thermal stability of powders

**3.2.1.1. Influence of the pyrolysis temperature.** TGA experiments were carried on powders synthesized at 1200 and 1400 °C (Fig. 5). Results confirm that the pyrolysis temperature of the aluminosilazane has a great influence on the powder thermal stability. The powder fabricated at 1400 °C does not present a mass loss up to 1200 °C. On the contrary, the temperature of 1200 °C is too low because it implies a mass loss of about 10 wt.% after a post-treatment at 700 °C. We can distinguish two domains, one between 100 and 400 °C, and the other in the range 500–700 °C. This lower thermal stability is certainly due to an uncomplete decomposition of the precursor in the reactional zone. Other authors have previously reported that the mass loss, occurring during the post-treatment, was mainly due to a gaseous release of ammonia, methane and dihydrogen.<sup>18,31,32</sup> This justifies the choice of 1400 °C for the pyrolysis temperature.

**3.2.1.2. Influence of the chemical composition.** The pyrolysis conditions directly influence the final composition of the powders, especially the carbon, nitrogen and aluminum contents. Therefore, TGA experiments (Fig. 6) were performed on different powders which compositions are given in Table 3, with a C/N

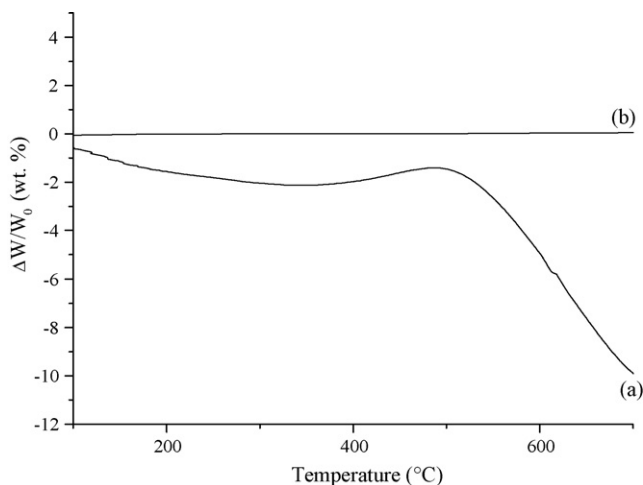


Fig. 5. TGA curves (in pure  $\text{N}_2$ ) of powders synthesized at 1200 °C (a) and 1400 °C (b).

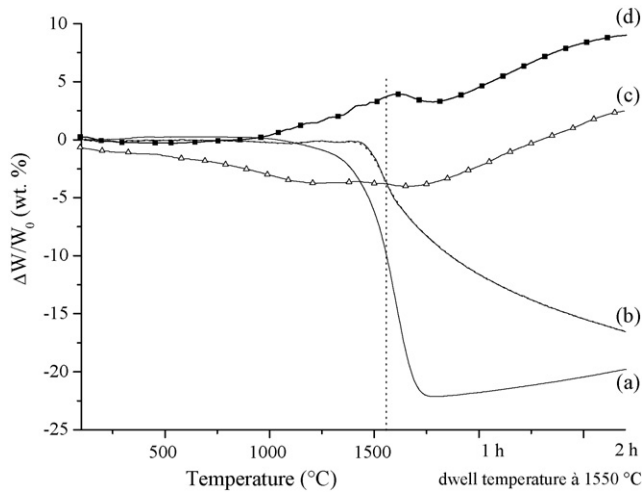


Fig. 6. TGA curves (treatment in 20% of N<sub>2</sub> in He) of as-synthesized powders with different C/N ratios: (a) 0.8, (b) 4.5, (c) 0.3 and (d) 0.2.

Table 3  
Mass loss evolution of the powders with their C/N ratio after TGA

C/N	C (wt.%)	Mass loss (%) <sup>*</sup>
4.5	45.8	≈17
0.8	22.5	≈22
0.8	21.8	≈21
0.3	7.6	≈4
0.2	5.4	–

ratio ranging from 0.2 to 4.5. For all the different batches, the mass loss is lower than 3–4 wt.% at 1450 °C, but above 1500 °C, their thermal behaviours differ. The more stable powders were fabricated in a reactive atmosphere (Ar/NH<sub>3</sub>). They present a small mass gain during the dwell temperature at 1550 °C. In Fig. 7, the mass changes after TGA treatment is shown versus the C/N molar ratio in the as-prepared powders. The batches characterized by C/N ratios higher than 0.2–0.3 exhibit a significant mass loss. During the pyrolysis of the aluminosilazane in a Ar/NH<sub>3</sub> atmosphere, there is a release of gaseous species containing carbon and nitrogen elements. The powders, containing free carbon with different contents, present a very low structural organisation characterized by groups such as Si–C–N–Si (Fig. 3), which are thermally unstable. Such groups were evi-

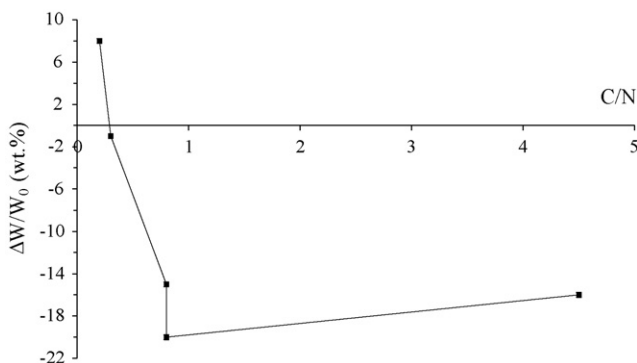


Fig. 7. Mass loss evolution after the TGA treatment vs. the powder C/N ratio.

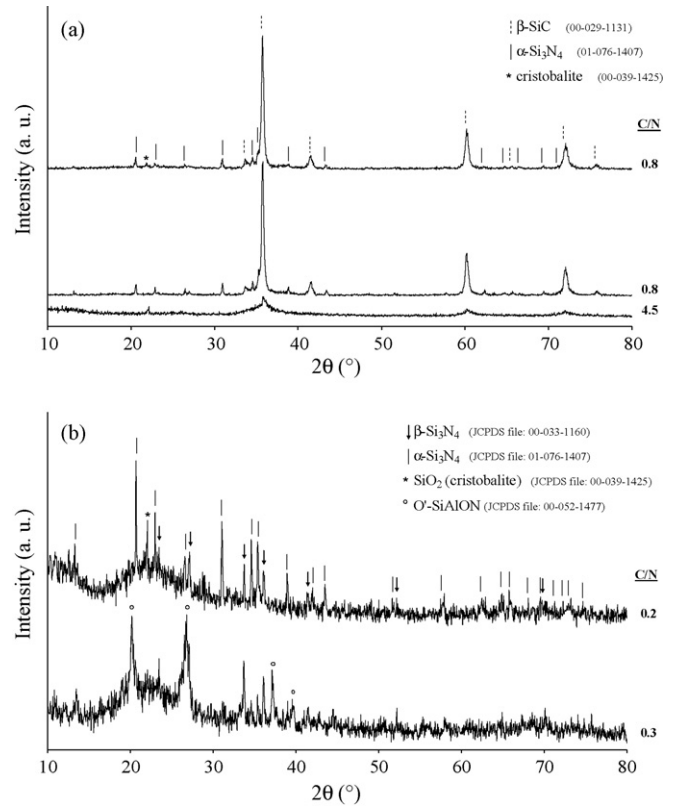
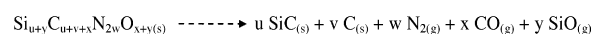


Fig. 8. (a) XRD diagrams of powders with C/N ≥ 0.8, after TGA treatment (10 °C min<sup>-1</sup>, 1550 °C, 2 h). (b) XRD diagrams of powders with C/N < 0.8, after TGA treatment (10 °C min<sup>-1</sup>, 1550 °C, 2 h).

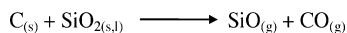
denced by Ténégal et al. by XAS in similar SiCN nanopowders, above 900 °C.<sup>42</sup> So, during the post-treatment, the powders go through important structural modifications. This structural reorganisation is related to the C/N ratio.

For C/N ≥ 0.8, the thermal stability of powders is limited. The most carbon-rich powder (C/N = 4.5) is stable up to 1400 °C, then it decomposes above. In the case of the powders with C/N = 0.8, the mass loss is detected from 900 °C but it stabilizes when the dwell temperature at 1550 °C is reached. The XRD patterns of these powders were registered after the TGA experiments (Fig. 8a). The main crystalline phase formed after the heat-treatment is β-SiC, but a smaller quantity of α-Si<sub>3</sub>N<sub>4</sub> is detected for the powder having a C/N ratio of 0.8.

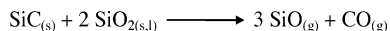
A lot of papers dealing with the thermal stability of SiCN solids, issued from the pyrolysis of polysilazanes, are published in literatures. The evolution of gaseous species containing nitrogen like HCN have been evidenced above 900 °C.<sup>24</sup> But the carbon and nitrogen losses from HCN release are certainly limited because there is few hydrogen in the powders. For higher temperatures, the decomposition of the Si<sub>w</sub>C<sub>x</sub>N<sub>y</sub>O<sub>z</sub> could lead to the formation of silicon carbide and free carbon, and to a decrease of the nitrogen content.<sup>4,43</sup> This reaction, illustrated in Scheme 2, takes place above 1484 °C at 1 atm,<sup>4</sup> and explains a mass loss detected by the TGA experiments. The silica phase



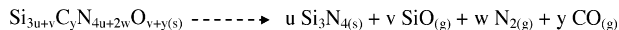
Scheme 2.



Scheme 3.



Scheme 4.



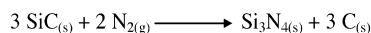
Scheme 5.

( $\alpha$ -cristobalite), present in low quantities, on the XRD patterns, could be due to a slight oxidation during the thermal treatment. It could also participate to the formation of gaseous species and to a mass loss (Schemes 3 and 4).

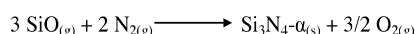
For  $C/N < 0.8$ , two batches of powders, corresponding to  $C/N = 0.2$  and  $0.3$ , were, respectively synthesized with a total gas flow rate of 3 and  $6 \text{ L min}^{-1}$ . The first one does not exhibit any mass loss, and the corresponding XRD pattern (Fig. 8b) presents the coexistence of both  $\alpha$ - and  $\beta$ -silicon nitride. This result is consistent with previous investigations which shows a silicon nitride formation, from an amorphous system with a  $C/N$  ratio of 0.2 (Scheme 5).<sup>24</sup> When the treatment dwell temperature is reached, the behaviour of this powder evolves similarly to that of powders containing more carbon (after pyrolysis in  $Ar/NH_3$ ). The TGA were realized in  $N_2/He$  (20/80), implying a very low partial pressure of oxygen. It is well known that a carbon loss can occur at low temperature with an evolution of  $CO_{(g)}$ , accompanied at higher temperature by the formation of  $SiO_{(g)}$ .<sup>43</sup> But the TGA curve of the batch of  $C/N = 0.2$  does not show any mass loss, thus it proves that there is no oxidation during the treatment. Therefore, the mass gain comes from powder nitridation, already identified by previous authors (Schemes 6 and 7).<sup>24,44</sup>

The as-synthesized powder, with a  $C/N = 0.3$  molar ratio, is rich in silicon nitride, and it also presents a SiAlON phase never detected in the other cases. This O'-SiAlON is derived from silicon oxynitride ( $Si_2N_2O$ ) which formation occurs at  $1400\text{--}1450^\circ\text{C}$  in  $N_2$ .<sup>45</sup> The phase should come from higher contents of aluminum (1.3 wt.%) and oxygen (4 wt.%) in this powder compared to the others. The aluminum content, twice higher than in the powder with a  $C/N = 0.2$ , seems to be sufficient to induce the crystallisation of such SiAlON phase in non-negligible quantity.

The ternary diagram, presented in Fig. 9, accounts for the changes of the powder compositions after post-treatments realized using the TGA device, 2 h at  $1550^\circ\text{C}$  in  $N_2/He$  atmosphere. The arrows illustrate the possible evolution of the composition, taking into account the crystalline phases detected by XRD in the different powders. Carbon-rich powders mainly evolve through silicon carbide (point 3) whereas nitrogen-rich powders preferentially lead to silicon nitride (point 6). Only the intermediate



Scheme 6.



Scheme 7.

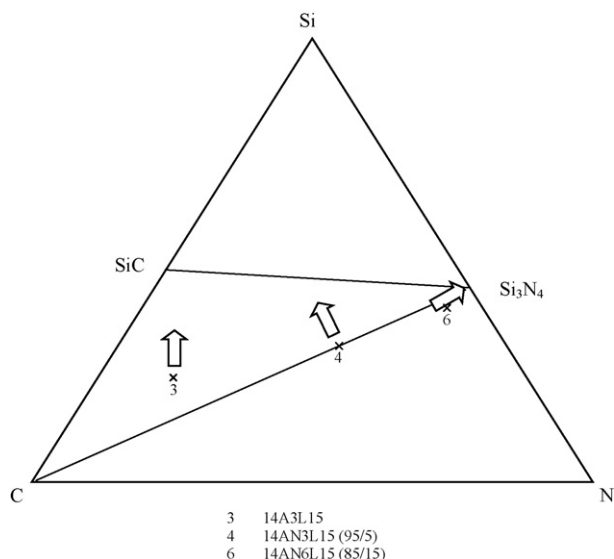


Fig. 9. Si–C–N ternary diagram involving the powder composition changes after a 2 h treatment at  $1550^\circ\text{C}$  in  $N_2/He$  (20/80).

compositions (point 4) should change in a  $Si_3N_4/SiC$  mixed system. We must notice that all the TGA experiments were carried out under a gas flow, so the gas composition is thought to be constant in the furnace treatment. Thus, the reactions presented in the different schemes are never considered at the thermodynamic equilibrium. However, these powders are more thermally stable than those synthesized from HMDS by laser pyrolysis in similar conditions.<sup>24</sup>

### 3.2.2. Sinterability

This part concerns preliminary tests to determine the sintering behaviour of these powders according to their initial composition.

The experiment was carried out by hot-pressing, in pure  $N_2$  at 1 atm, using a batch thermally stable ( $C/N = 0.3$ ), obtained with a flow rate of  $6 \text{ L min}^{-1}$ , and containing aluminum (1.3 wt.%). Fig. 10 shows the piston displacement versus the treatment temperature (or the experiment duration). The displacement depends on the expansion of the graphite and the compact, and on the pellet shrinkage during the heating. Above  $1400^\circ\text{C}$ , the

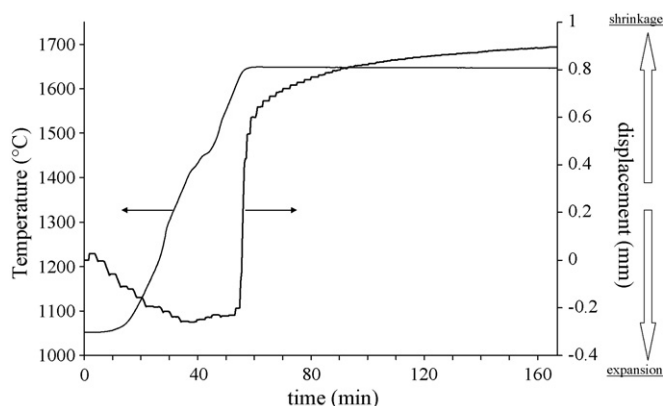


Fig. 10. Temperature and displacement during the hot-pressing experiment, for  $C/N = 0.3$  (batch: 14AN3L15 (95/5)).

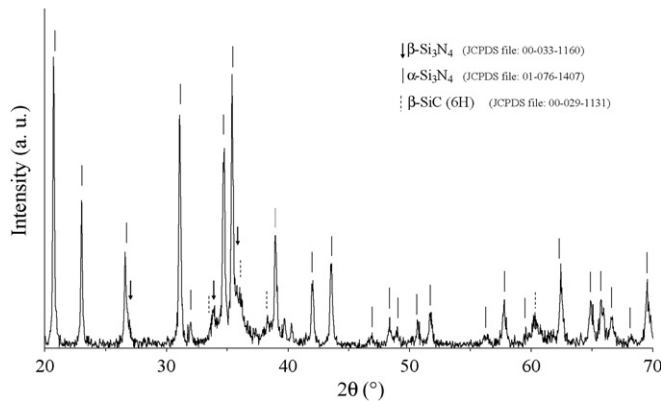
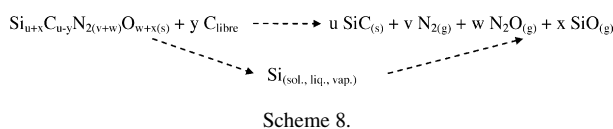


Fig. 11. XRD diagram of a powder, with a C/N ratio of 0.3 (batch: 14AN3L15 (95/5)), after a 2 h hot-pressing at 1650 °C (35 MPa, N<sub>2</sub>).

displacement signal evolves, indicating shrinkage of the sample with a maximum rate around 1600–1650 °C. The last step, during the dwell temperature, consists in a low and continuous shrinkage, which is certainly due to an incomplete densification. This behaviour is similar to that of a mixture containing SiCN obtained by laser pyrolysis of HMDS, alumina (3 wt.%) and yttria (6 wt.%) powders.<sup>24</sup> The study showed a shrinkage of the pellet from 1500 to 1700 °C. Thus, the fast shrinkage, measured in the range 1600–1650 °C, should correspond to a viscous behaviour linked to the presence of aluminum and oxygen, distributed in the bulk of the particles, which would favour the particles rearrangement at the beginning of the sintering step. After having removed the pellet from the mould, we observed that it presented a low densification. The corresponding XRD pattern (Fig. 11) shows that α-Si<sub>3</sub>N<sub>4</sub> was mainly present compared to β-Si<sub>3</sub>N<sub>4</sub> and β-SiC phases. The sintering experiment was carried out in a nearly closed nitrogen atmosphere ( $P = 1$  atm), and therefore, the compositional changes are more limited than in the case of TGA measurements. The viscosity of the material, which decreases during the thermal treatment, is too high to allow the total densification. No new crystalline phase, containing aluminum, nitrogen, silicon and oxygen elements, was detected after cooling (Fig. 11).

Other experiments were carried out using a spark plasma sintering (SPS) system under vacuum (Dr. Sinter 2080, Sumitomo Coal Mining Company, Japan). This device allowed to use a heating rate higher than 50 °C min<sup>-1</sup> to preserve a fine microstructure, but the final densities obtained were similar to those obtained by hot-pressing. Some gaseous evolutions were detected during the sintering experiments, certainly due to a partial decomposition of the oxycarbonitride particles favoured by the vacuum atmosphere. The microstructures obtained were logically rich in silicon carbide which formation could be explained by the decomposition of the silicon oxycarbonitride phase, Si<sub>w</sub>C<sub>x</sub>N<sub>y</sub>O<sub>z</sub>, according to Scheme 8.<sup>43</sup> The decomposition phe-



nomenon and the weak presence of oxygen and aluminum have a deleterious effect on the sintering behaviour of the material.

To avoid this detrimental effect, as shown previously, experiments should be carried out at 1 atm with a nitriding atmosphere.

#### 4. Conclusions

The thermal stability of SiCNAIO nanopowders strongly depends on their crystallisation degree, but also on their stoichiometry. In this paper, we evidenced that the C/N ratio value is very important to control both the thermal stability and the nature of phases, which appear after a post-pyrolysis heat-treatment. The use of a reactive atmosphere, with Ar/NH<sub>3</sub> mixtures, allowed to obtain powders containing C/N molar ratios in the range 0.1–4.5 for rates of ammonia of 25–0 wt.%. The introduction of ammonia in the pyrolysis atmosphere induces a stabilization of the Al–N bond, and the thermal stability of as-synthesized powders is higher than that of powders produced from laser-pyrolysis (using similar pyrolysis parameters).<sup>25</sup> The preliminary tests of powder sinterability showed that the densification was promoted by a viscous behaviour of the material due to the presence of both aluminum and oxygen.

Experiments are in progress to introduce yttrium in the precursor, the presence of higher quantity of heteroelements in the material would favour its total densification.

#### Acknowledgements

The authors wish to thank E. Laborde for his technical help on the pyrolysis set-up (SPCTS, Université de Limoges, France), D. Tétard for the high-pressure sintering tests (SPCTS) and P. Gaveau for the solid NMR analyses (GDPC, Université Montpellier II, France).

#### References

- Wen, G., Li, F. and Song, L., Structural characterization and mechanical properties of SiBONC ceramics derived from polymeric precursors. *Mater. Sci. Eng. A*, 2006, **432**, 40–46.
- Sato, K., Saitoh, T., Nagano, T. and Iwamoto, Y., Low temperature crystallization behaviour of alpha-Si<sub>3</sub>N<sub>4</sub> from Ti-doped amorphous silicon nitride derived from polytitanasilazanes. *J. Ceram. Soc. Jap.*, 2006, **114**(6), 502–506.
- Narisawa, M., Tanno, H., Ikeda, M., Iseki, T., Mabuchi, H., Okamura, K. et al., Synthesis and ceramization of polymethylsilane precursors modified with metal chlorides. *J. Ceram. Soc. Jap.*, 2006, **114**(6), 558–562.
- Horz, M., Zern, A., Berger, F., Haug, J., Muller, K., Aldinger, F. et al., Novel polysilazanes as precursors for silicon nitride/silicon carbide composites without “free” carbon. *J. Eur. Ceram. Soc.*, 2005, **25**, 99–110.
- Schiavon, M. A., Sorarù, G. D. and Yoshida, I. V. P., Poly(borosilazanes) as precursors of Si–B–C–N glasses: synthesis and high temperature properties. *J. Non-Cryst. Solids*, 2004, **348**, 156–161.
- Hapke, J. and Ziegler, G., Synthesis and pyrolysis of liquid organometallic precursors for advanced Si–Ti–C–N composites. *Adv. Mater.*, 1995, **7**(4), 380–384.
- Li, Y., Zheng, Z., Reng, C., Zhang, Z., Gao, W., Yang, S. et al., Preparation of Si–C–N–Fe magnetic ceramics from iron-containing polysilazane. *Appl. Organomet. Chem.*, 2003, **17**, 120–126.
- Iwamoto, Y., Kikuta, K.-I. and Hirano, S.-I., Microstructural development of Si<sub>3</sub>N<sub>4</sub>–SiC–Y<sub>2</sub>O<sub>3</sub> ceramics derived from polymeric precursors. *J. Mater. Res.*, 1998, **13**(2), 353–361.

9. Babonneau, F., Soraru, G. D., Thorne, K. J. and Mackenzie, J. D., Chemical characterization of Si–Al–C–O precursor and its pyrolysis. *J. Am. Ceram. Soc.*, 1991, **74**(7), 1725–1728.
10. Soraru, G. D., Ravagni, A., Campostrini, R. and Babonneau, F., Synthesis and characterization of beta'-SiAlON ceramics from organosilicon polymers. *J. Am. Ceram. Soc.*, 1991, **74**(9), 2220–2223.
11. Seyferth, D., Brodt, G. and Boury, B., Polymeric aluminasilazane precursors for aluminosilicon nitride. *J. Mater. Sci. Lett.*, 1996, **15**, 348–349.
12. Verdecia, G., O'Brien, K. L., Schmidt, W. R. and Apple, T. M., Aluminum-27 and silicon-29 solid-state nuclear magnetic resonance study of silicon carbide/aluminum nitride systems: effect of silicon/aluminum ratio and pyrolysis temperature. *Chem. Mater.*, 1998, **10**, 1003–1009.
13. Boury, B. and Seyferth, D., Preparation of Si/C/Al/N ceramics by pyrolysis of polyaluminasilazanes. *Appl. Organomet. Chem.*, 1999, **13**, 431–440.
14. Berger, F., Weinmann, M., Aldinger, F. and Muller, K., Solid-state NMR studies of the preparation of Si–Al–C–N ceramics from aluminum-modified polysilazanes and polysilylcarbodiimides. *Chem. Mater.*, 2004, **16**, 919–929.
15. Yajima, S., Hasegawa, Y., Okamura, K. and Matsuzawa, T., Development of high tensile strength silicon carbide fibre using an organosilicon polymer precursor. *Nature*, 1978, **273**, 525–527.
16. Seyferth, D. and Plenio, H., Borasilazane polymeric precursors for borosilicon nitride. *J. Am. Ceram. Soc.*, 1990, **73**(7), 2131–2133.
17. Funayama, O., Kato, T., Tashiro, Y. and Isoda, T., Synthesis of a polyborosilazane and its conversion into inorganic compounds. *J. Am. Ceram. Soc.*, 1993, **76**(3), 717–723.
18. Funayama, O., Nakahara, H., Okoda, M., Okumura, M. and Isoda, T., Conversion mechanism of polyborosilazane into silicon nitride-based ceramics. *J. Mater. Sci.*, 1995, **30**, 410–416.
19. Riedel, R., Kienzle, A., Dressler, W., Ruwisch, L., Bill, J. and Aldinger, F., A silicoboron carbonitride ceramic stable to 2000 °C. *Nature*, 1996, **382**, 796–798.
20. Schmidt, W. R., Narsavage-Heald, D. M., Jones, D. M., Marchetti, P. S., Raker, D. and Maciel, G. E., Poly(borosilazane) precursors to ceramic nanocomposites. *Chem. Mater.*, 1999, **11**, 1455–1464.
21. Janakiraman, N., Weinmann, M., Schuhmacher, J., Muller, K., Bill, J. and Aldinger, F., Thermal stability, phase evolution, and crystallization in Si–B–C–N ceramics derived from a polyborosilazane precursor. *J. Am. Ceram. Soc.*, 2002, **85**(7), 1807–1814.
22. Bernard, S., Fiaty, K., Cornu, D., Miele, P. and Laurent, P., Kinetic modeling of the polymer-derived ceramics route: investigation of the thermal decomposition kinetics of polyB-(methylamino)borazine precursors into boron nitride. *J. Phys. Chem. B*, 2006, **110**, 9048–9060.
23. Salles, V., Foucaud, S., Laborde, E., Champion, E. and Goursat, P., Synthesis of SiCNAI(O) pre-alloyed nanopowders by pyrolysis of an aluminosilazane aerosol. *J. Eur. Ceram. Soc.*, 2007, **27**(1), 357–366.
24. Doucey, B., *Nanocomposites Si<sub>3</sub>N<sub>4</sub>/SiC: Stabilité thermique et densification de poudres SiCN(Al,O) synthétisées par pyrolyse laser; Comportement au fluage des frittés*. Ph.D. Thesis, Limoges, 1999.
25. Dez, R., Ténégal, F., Reynaud, C., Mayne, M., Armand, X. and Herlin-Boime, N., Laser synthesis of silicon carbonitride nanopowders, structure and thermal stability. *J. Eur. Ceram. Soc.*, 2002, **22**(16), 2969–2979.
26. Balhoul-Hourlier, D., Doucey, B., Laborde, E. and Goursat, P., Investigations on thermal reactivity of Si/C/N nanopowders produced by laser aerosol or gas interactions. *J. Mater. Chem.*, 2001, **11**, 2028–2034.
27. Birot, M., Pillot, J. P. and Dunogues, J., Comprehensive chemistry of polycarbosilanes, polysilazanes, and polycarbosilazanes as precursors of ceramics. *Chem. Rev.*, 1995, **95**(5), 1443–1477.
28. Burns, G. T. and Chandra, G., Pyrolysis of preceramic polymers in ammonia: preparation of silicon nitride powders. *J. Am. Ceram. Soc.*, 1989, **72**(2), 333–337.
29. Corriu, R. J. P., Leclercq, D., Mutin, P. H. and Vioux, A., Thermogravimetric mass spectrometric investigation of the thermal conversion of organosilicon precursors into ceramics under argon and ammonia 1. poly(carbosilane). *Chem. Mater.*, 1992, **4**, 711–716.
30. Lavedrine, A., *Etude de la décomposition de polysilazanes; Comportement à l'oxydation du carbonitride de silicium obtenu*. Ph.D. Thesis, Université de Limoges, 1991.
31. Musset E., *Synthèse de poudres nanométriques à base de silicium, carbone et azote par couplage aérosol-laser et leurs caractérisations*. Ph.D. Thesis, Paris XI Orsay, 1995.
32. Salvetti, M. G., Pijolat, M., Soustelle, M. and Chassagneux, E., Pyrolysis of a polysilazane precursor to SiCN ceramics. *Solid State Ionics*, 1993, **63–65**, 332–339.
33. Soucy, G., Jurewicz, J. W. and Boulos, M. I., Parametric study of the decomposition of NH<sub>3</sub> for an induction plasma reactor design. *Plasma Chem. Plasma Proc.*, 1995, **15**(4), 693–710.
34. Soucy, G., Jurewicz, J. W. and Boulos, M. I., Parametric study of the plasma synthesis of ultrafine silicon nitride powders. *J. Mater. Sci.*, 1995, **30**, 2008–2018.
35. Rice, G. W., Laser synthesis of silicon/carbon/nitrogen powders from 1,1,1,3,3,3-hexamethyldisilazane. *J. Am. Ceram. Soc.*, 1986, **69**(8), C183–C185.
36. He, X.-M., Shu, L., Li, W.-Z. and Li, H.-D., Structure and properties of carbon nitride films synthesized by low energy ion bombardment. *J. Mater. Res.*, 1997, **12**(6), 1595–1602.
37. Jelinek, M., Zemek, J., Trchova, M., Vorlicek, V., Lancok, J., Tomov, R. et al., CN<sub>x</sub> films created by combined laser deposition and r.f. discharge: XPS, FTIR and Raman analysis. *Thin Solid Films*, 2000, **366**, 69–76.
38. Wei, A., Chen, D., Ke, N., Peng, S. and Wong, S. P., Characteristics of carbon nitride films prepared by magnetic filtered plasma stream. *Thin Solid Films*, 1998, **323**, 217–221.
39. Balhoul-Hourlier, D., Doucey, B., Besson, J.-L. and Goursat P., In *Thermal reactivity of silicon-based nanopowders* ed. Legrand, A.P. and Sénémaud C., London, 2003 pp.41–53.
40. Salles, V., *Nanopoudres multiéléments SiCNAIO à partir d'un aérosol d'aluminosilazane: Synthèse et comportement thermique*. Ph.D. Thesis, 2006.
41. Legrand, A.P., d'Espinose de la Caillerie, J.B. and El Kortobi, Y., In *Chemical order studied by solid-state nuclear magnetic resonance* ed. Legrand, A.P. and Sénémaud, C., London, 2003.
42. Ténégal, F., Flank, A.-M. and Herlin, N., Short-range atomic-structure description of nanometric Si/C/N powders by X-ray-absorption spectroscopy. *Phys. Rev. B*, 1996, **54**(17), 12029–12035.
43. Pereira M., *Stabilité thermique et comportement à l'oxydation des céramiques à base de carbonitride de silicium issues de la pyrolyse de précurseurs polyvinylsilazanes*. Ph.D. Thesis, Université de Limoges, 1994.
44. Mayne, M., Balhoul-Hourlier, D., Doucey, B., Goursat, P., Cauchetier, M. and Herlin, N., Thermal behaviour of sicn nanopowders issued from laser pyrolysis. *J. Eur. Ceram. Soc.*, 1998, **18**, 1187–1194.
45. Goursat, P., Lortholary, P. and Billy, M., Etude du système silicium-oxygène-azote, 1-préparation de l'oxynitride Si<sub>2</sub>N<sub>2</sub>O. *Rev. Int. Hautes Temp. Réfract.*, 1971, **8**, 149–154.